

# **A theoretical framework for calibrating the transversely isotropic elastic rock parameters from UCS tests on cylindrical specimens using circumferential strain measurements**

Manuel Bernhard Winkler

*Graz University of Technology, Institute of Rock Mechanics and Tunnelling, Graz, Austria*

Thomas Frühwirt

*Graz University of Technology, Institute of Rock Mechanics and Tunnelling, Graz, Austria*

Thomas Marcher

*Graz University of Technology, Institute of Rock Mechanics and Tunnelling, Graz, Austria*

**ABSTRACT:** The standard method for determining the set of five independent elastic constants of transversely isotropic rocks relies on the conduction of at least three UCS tests with directional radial strain measurements on samples with varying isotropy plane orientation. However, in many cases only averaged values for the lateral strains are available from chain extensometer measurements as commonly carried out in rock mechanics laboratories. Such measurement setups disregard the anisotropic deformational behavior of transversely isotropic rock samples which appears as a result of non-horizontal isotropy plane orientations. A direct utilization of averaged radial strains in the determination of the five independent parameters without further considerations is thus not possible. In this paper a possible scheme for the inclusion of circumferential strain measurement information in the determination of the elastic constants of transversely isotropic rocks based on UCS tests carried out on three samples with varying isotropy plane inclinations is presented.

*Keywords: UCS tests, transverse isotropy, elastic parameters, circumferential strain measurement, Poisson's ratio.*

## **1 INTRODUCTION**

A common assumption made in modelling the elastic deformational behavior of rocks with distinct planar structures (i.e., bedding, foliation, schistosity) is the assumption over transverse isotropy. Thereby, a plane of isotropy is assumed to be present parallel to the rock layering. Transversely isotropic materials feature five independent elastic parameters (Lekhnitskii 1981): The Young's moduli  $E$  and  $E'$  in directions parallel and normal to the planes of isotropy; the Poisson's ratios  $\nu$  and  $\nu'$ , referring to the lateral strains within the isotropy plane following normal strains applied in plane-parallel and plane-normal directions; and the shear modulus  $G'$  connected to shear deformations in the plane of isotropy for shear loading in this plane.

In literature different methods are proposed to determine these elastic parameters. While some of them rely on rather extraordinary test setups using specially shaped specimens and uncommon boundary conditions (e.g. Talesnick & Ringel 1999) some methods utilize standardized procedures, such as the uniaxial compression test (Amadei 1996, Barla 1972). As can be proven by theoretical

considerations, it is not possible to exactly determine all elastic constants by only one single uniaxial compression test (Nejati et al. 2019). Thus, either the approximate determination of unknown constants is mandatory or multiple tests on several specimens with varying isotropy plane inclinations need to be performed. The Poisson's ratios and/or the independent shear modulus have to be calibrated based on lateral strain measurements in specific polar orientations along the sample circumference. However, due to difficulties associated with applying strain gauges especially to softer rock specimens, connected with poor surface adhesion, and the fact that alternative diametral strain extensometer setups are not readily available in many rock mechanics laboratories, directional measurements of lateral strains are often not feasible. Instead, lateral strains are frequently recorded in an averaged way on the basis of circumferential strain measurements using chain extensometers.

In this study therefore a novel way of including the circumferential strain measurements in the evaluation of the set of elastic transversely isotropic constants is suggested. Section 2 provides theoretical background information. In section 3 the proposed framework for the determination of the elastic constants based on circumferential strain measurements is presented. The final section 4 includes a condensed summary of the key points of the new procedure, discusses its limitations and presents and outlook for future studies.

## 2 THEORETICAL BACKGROUND

### 2.1 Cylindrical coordinate system

All presented mathematical evaluations in this paper refer to a cylindrical coordinate system with the  $z$ -axis corresponding to the axes of the cylindrical specimens. The polar orientation  $\theta$  of a point along the sample circumference at measuring cross-section level is chosen to be equal to the angle between the polar point direction and the Cartesian  $x$ -axis (oppositely oriented to the isotropy plane dip direction). The latter also defines the direction of a symmetry plane for transversely isotropic samples with respect to generated stresses and strains during axial loading (Dambly et al. 2019). Symbol  $\beta$  designates the isotropy plane dip angle. A graphical representation of the chosen cylindrical coordinate system and the reference Cartesian  $x$ - $y$ -system is shown in Figure 1.

### 2.2 Standard calibration procedure

In order to calibrate the elastic constants of transversely isotropic cylindrical samples from UCS tests, the measured values for axial and oriented radial strains in the measuring cross-section must be correlated with theoretical strain equations (Barla 1972). These equations are derived from mathematical transformations of the generalized Hook's law considering a transversely isotropic compliance matrix. In total, five equations for the five unknown elastic constants must be defined from three tests carried out in normal, parallel and inclined directions to the samples' isotropy planes. The general equations of the normalized axial ( $\varepsilon_z$ ) and radial ( $\varepsilon_r$ ) strains of circumferential points on the measuring cross-section, in dependency of the elastic constants, the isotropy plane inclination  $\beta$  and polar orientation  $\theta$ , are as follows (Dambly et al. 2019):

$$\frac{\varepsilon_r}{\sigma_z} = \left( -\frac{\nu \sin^2 \beta}{E} - \frac{\nu' \cos^2 \beta}{E'} \right) \sin^2 \theta + \frac{1}{4} \left[ \left( \frac{1}{E} - \frac{1}{G'} + \frac{1}{E'} \right) \sin^2 2\beta - \frac{\nu'(3 + \cos 4\beta)}{E'} \right] \cos^2 \theta \quad (1)$$

$$\frac{\varepsilon_z}{\sigma_z} = \frac{\sin^4 \beta}{E} + \frac{\cos^4 \beta}{E'} + \frac{1}{4} \left( \frac{1}{G'} - \frac{2\nu'}{E'} \right) \sin^2 2\beta \quad (2)$$

Provided that samples with isotropy plane inclinations of  $\beta = 0^\circ$ ,  $45^\circ$  and  $90^\circ$  are used in the calibration of the elastic constants and that the orientations of radial strain measurements correspond to polar orientations  $\theta = 0^\circ$  for the samples with  $\beta = 0^\circ$  and  $45^\circ$  and  $\theta = 90^\circ$  for the sample with  $\beta = 90^\circ$ , more simplified equations can be obtained from Eqns. (1) to (2) (see Alejano et al. 2021). Eqns. (1) to (2) can be used to determine the elastic constants by replacing the equations' left-hand sides with the measured values from the tests. Figure 1 provides an overview on the sequential steps in the standard calibration procedure and the directions for the radial strain measurements to be considered.

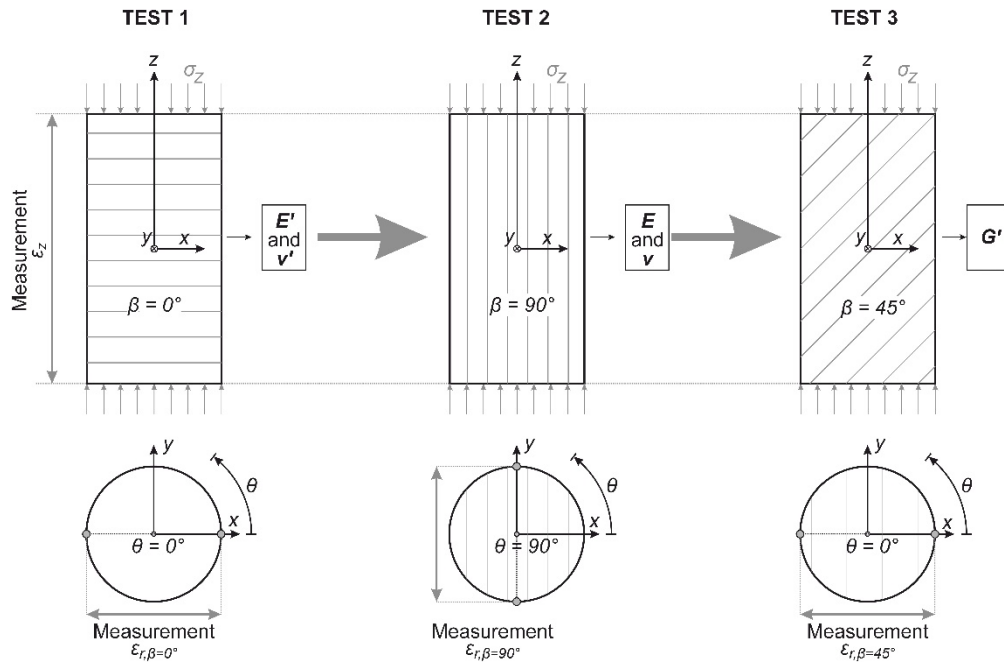


Figure 1. Standard calibration procedure for the transversely isotropic elastic parameters and considered coordinate systems.

### 3 PROPOSED CALIBRATION PROCEDURE

The proposed methodology for the parameter calibration refers to the evaluation of the stress-strain curves on conducted unloading-reloading (UR) cycles. Due to the theoretical direction-independent uniform distribution of radial strains for samples with horizontal planes of isotropy ( $\beta = 0^\circ$ ), the radial strains  $\epsilon_r$  for these samples can be inferred from the measurement of the circumferential strains  $\epsilon_c$  using a chain extensometer ( $\epsilon_r = \epsilon_c$ ). The Young's modulus  $E'$  and Poisson's ratio  $\nu'$  can then simply be computed from Eqns. (1) and (2). The determination of Young's modulus  $E$  is independent of any lateral strain measurement and is further accomplished from the information on the axial strain for samples with  $\beta = 90^\circ$  inserted into Eqn. (2). The shear modulus  $G'$  can be received from the axial strain measurement of samples with inclined planes of isotropy ( $\beta = 45^\circ$ ) by invoking Eqn. (2). To come up with the derived value for the Poisson's ratio  $\nu$ , circumferential strain measurements of tests on samples with inclined and vertical planes of isotropy will both be incorporated. An optimization problem is set up with the aim of minimizing the differences in the measured and theoretical values for circumferential strains, determined as the change in circumference of assumed elliptical cross-sections of the samples at the lower bound  $\sigma_{LB}$  and upper bound  $\sigma_{UB}$  stress levels of the UR cycles. The assumption is followed that the samples retain the circular initial geometry, when the load along the unloading path is reduced to zero. Thus, any influence of plastic deformations on the cross-sectional shape of the samples is neglected in the evaluation of theoretical circumferential strains.

### 3.1 Theoretical cross-section geometries - sample with $\beta = 90^\circ$

From the assumption of a circular cross-section in the case of complete unloading, the main axes of the elliptical cross section at stress level  $\sigma_{LB}$  are given by  $x_{90}$  and  $y_{90}$  with  $y_{90} = K_{90}x_{90}$ . Length  $x_{90}$  is determined from the initial radius  $r$  plus the amount of elastic deformations (derived from Eqn. 1) from zero stress to the lower bound stress level  $\sigma_{LB}$  as  $x_{90} = r \cdot (1 + \nu'/E' \cdot \sigma_{LB})$ . Length  $y_{90}$  is dependent on the unknown Poisson's ratio  $\nu$  and is given by  $y_{90} = r \cdot (1 + \nu/E \cdot \sigma_{LB})$ . Factor  $K_{90}$  can then be computed as the ratio of  $y_{90}/x_{90}$  (Eqn. 3). The main axes of the ellipse at the upper bound stress level  $\sigma_{UB}$  are received from adding the theoretical elastic deformations  $\Delta x_{90}$  and  $\Delta y_{90}$ , following a stress increase by  $\Delta\sigma = \sigma_{UB} - \sigma_{LB}$ , to the values for  $x_{90}$  and  $y_{90}$ , whereby  $\Delta y_{90} = Q_{90}\Delta x_{90}$ . The length changes compute as  $\Delta x_{90} = r \cdot \nu'/E' \cdot \Delta\sigma$  (known) and  $\Delta y_{90} = r \cdot \nu/E \cdot \Delta\sigma$  (unknown). Factor  $Q_{90}$  is presented in Eqn. (3).

$$K_{90} = \frac{1 + \frac{\nu}{E} \cdot \sigma_{LB}}{1 + \frac{\nu'}{E'} \cdot \sigma_{LB}}, \quad Q_{90} = \frac{\nu E'}{\nu' E} \quad (3)$$

Figure 2 provides an overview of the considered parts and stress levels of the stress-strain curve for the evaluation of the elastic parameters and the theoretical assumption on the cross-sectional shapes of the measuring cross section at these various stress levels.

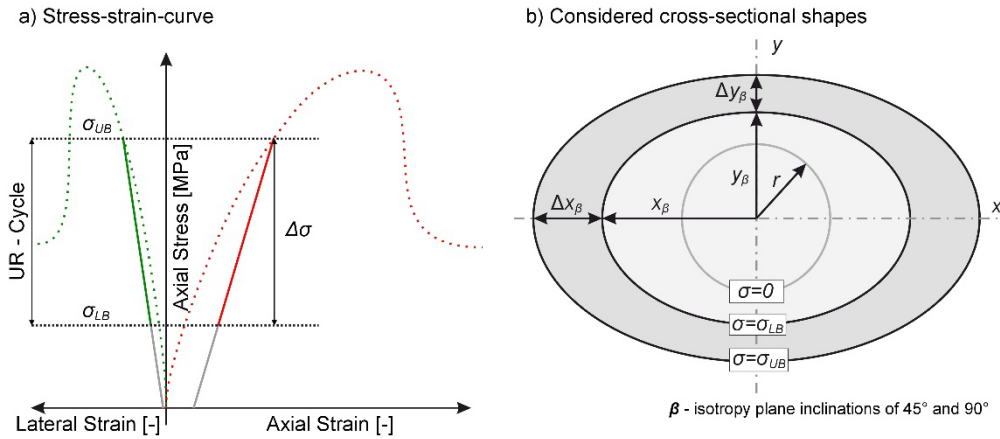


Figure 2. a) Considered stress levels along the UR-cycles of the stress strain curves and b) associated cross-sectional geometries.

### 3.2 Theoretical cross-section geometries - sample with $\beta = 45^\circ$

The considerations for the evaluation of the cross-sectional geometry of the sample at lower and upper bound stress levels  $\sigma_{LB}$  and  $\sigma_{UB}$  are the same as described in section 3.1 for samples with  $\beta = 90^\circ$ . The only difference is the value of  $\beta$  to be considered in the interpretation of the elastic strains, elastic deformations respectively, following Eqn. (1). For samples with  $\beta = 45^\circ$ , the initial axes  $x_{45}$  at stress level  $\sigma_{LB}$  and the length change  $\Delta x_{45}$ , following a stress increase by  $\Delta\sigma$ , are given as stated below:

$$x_{45} = r \left( 1 + \frac{1}{4} \left[ \left( \frac{1}{G'} - \frac{1}{E} - \frac{1}{E'} \right) + \frac{2\nu'}{E'} \right] \cdot \sigma_{LB} \right) \quad (4)$$

$$\Delta x_{45} = \frac{r}{4} \left[ \left( \frac{1}{G'} - \frac{1}{E} - \frac{1}{E'} \right) + \frac{2\nu'}{E'} \right] \cdot \Delta\sigma \quad (5)$$

Eqns. (4) and (5) are independent of the unknown Poisson's ratio  $\nu$  and can be evaluated with the already known information. The relationships for the initial axis length  $y_{45}$  and length change  $\Delta y_{45}$  are established as  $y_{45} = K_{45}x_{45}$  and  $\Delta y_{45} = Q_{45}\Delta x_{45}$  with factors  $K_{45}$  and  $Q_{45}$  as given in Eqn. (6).

$$K_{45} = \frac{1 + \frac{1}{2} \left( \frac{\nu}{E} + \frac{\nu'}{E'} \right) \cdot \sigma_{LB}}{1 + \frac{1}{4} \left[ \left( \frac{1}{G'} - \frac{1}{E} - \frac{1}{E'} \right) + \frac{2\nu'}{E'} \right] \cdot \sigma_{LB}}, \quad (6)$$

$$Q_{45} = \frac{\frac{1}{2} \left( \frac{\nu}{E} + \frac{\nu'}{E'} \right)}{\frac{1}{4} \left[ \left( \frac{1}{G'} - \frac{1}{E} - \frac{1}{E'} \right) + \frac{2\nu'}{E'} \right]}$$

### 3.3 Ellipse perimeter and theoretical circumferential strains

For computing the theoretical perimeter  $p$  of the elliptical cross sections of the samples at various stress levels, based on the geometrical relationships for the semi axes length  $(x, y)$  discussed in sections 3.1 and 3.2, an approximation by Linderholm & Segal (1995), considering the effective radius  $r'$ , is used.

$$p = 2\pi r' \quad \text{with} \quad r' = \left( \frac{x^{3/2} + y^{3/2}}{2} \right)^{2/3} \quad (7)$$

Using Eqn. (7), the perimeter of the assumed elliptical cross-sections for samples with various isotropy plane inclinations  $\beta$  ( $45^\circ, 90^\circ$ ) at the lower stress level  $\sigma_{LB}$  can be computed as

$$p_{LB,\beta} = 2\pi \left( \frac{x_\beta^{3/2} + (K_\beta x_\beta)^{3/2}}{2} \right)^{2/3} \quad (8)$$

and at the upper bound stress level  $\sigma_{UB}$  as

$$p_{UB,\beta} = 2\pi \left( \frac{(x_\beta + \Delta x_\beta)^{3/2} + (K_\beta x_\beta + Q_\beta \Delta x_\beta)^{3/2}}{2} \right)^{2/3} \quad (9)$$

Then, the theoretical circumferential strains in relation to the initial sample geometry with radius  $r$  can be calculated as

$$\varepsilon_{c,\beta}^* = \frac{p_{UB,\beta} - p_{LB,\beta}}{2r\pi} \quad (10)$$

### 3.4 Optimization process

The actual value for Poisson's ratio  $\nu$  is found from the solution of a non-linear optimization problem with a defined objective function to be minimized. The objective function is defined depending on the sum of the squared errors between the measured strains  $\varepsilon_{c,UR,\beta}$  and the theoretical circumferential strains  $\varepsilon_{c,\beta}^*$  acc. to Eqn. (9).

$$f(\nu) = \sqrt{\sum_{\beta} (\varepsilon_{c,UR,\beta} - \varepsilon_{c,\beta}^*)^2} \quad \text{with } \beta = 45^\circ \text{ and } 90^\circ \quad (11)$$

The optimization problem can be solved with any of the available non-linear optimization algorithms. Bounds can be set on the variable  $\nu$  to prevent solutions outside the realistic range.

#### 4 SUMMARY AND OUTLOOK

In this paper a theoretical framework for the evaluation of the transversely isotropic parameters based on 3 UCS tests performed on samples with horizontal, inclined and vertical planes of isotropy including circumferential strain measurements has been developed. For the evaluation of the theoretical circumferential strains of the samples within unloading-reloading cycles the assumption of cross-sectional ellipticity has been made. The elliptical geometries of the cross-sections at various stress levels have been determined based on the initial sample geometry and the considered load levels causing elastic deformations as derived from the theory of anisotropic elasticity. The perimeters of the deformed cross-sections have been approximated by the determination of an effective radius for the corresponding ellipses. An objective function in dependency of Poisson's ratio  $\nu$  has been defined including measured and theoretical values for the circumferential strains. The calibration of this parameter has been suggested to follow from the solution of an associated non-linear optimization problem.

So far, the proposed frame work has not been extensively employed on test results from anisotropic rock samples. Due to the neglect of plastic deformations in the considerations for the cross-sectional geometries the adoption of the described calibration procedure might be limited to rocks with a minor plastic behavior or UR-cycles performed at low stress levels. Further, the involved approximations of the ellipse perimeters might cause inaccuracies in the final values for the Poisson's ratio  $\nu$ . It is the aim of future studies to investigate the practical applicability of the proposed method and to quantify the involved uncertainties.

#### REFERENCES

- Alejano, L. R., González-Fernández, M. A., Estévez-Ventosa, X., Song, F., Delgado-Martín, J., Muñoz-Ibáñez, A., González-Molano, N., & Alvarillos, J. 2021. Anisotropic deformability and strength of slate from NW-Spain. *International Journal of Rock Mechanics and Mining Sciences*, 148, 104923. <https://doi.org/10.1016/j.ijrmms.2021.104923>
- Amadei, B. 1996. Importance of anisotropy when estimating and measuring in situ stresses in rock. *International Journal of Rock Mechanics and Mining Sciences & Geomechanics Abstracts*, 33(3), 293–325. [https://doi.org/10.1016/0148-9062\(95\)00062-3](https://doi.org/10.1016/0148-9062(95)00062-3)
- Barla, G. 1972. Rock Anisotropy: Theory and Laboratory Testing. In L. Müller (Ed.), *Rock Mechanics* (pp. 131–169). Springer Vienna. [https://doi.org/10.1007/978-3-7091-4109-0\\_8](https://doi.org/10.1007/978-3-7091-4109-0_8)
- Dambly, M. L. T., Nejati, M., Vogler, D., & Saar, M. O. 2019. On the direct measurement of shear moduli in transversely isotropic rocks using the uniaxial compression test. *International Journal of Rock Mechanics and Mining Sciences*(113), 220–240. <https://doi.org/10.1016/j.ijrmms.2018.10.025>
- Lekhnitskii, S. G. 1981. *Theory of Elasticity of an Anisotropic Body*. MIR Publishers.
- Linderholm, C. E., & Segal, A. C. 1995. An Overlooked Series for the Elliptic Perimeter. *Mathematics Magazine*, 68(3), 216. <https://doi.org/10.2307/2691422>
- Nejati, M., Dambly, M. L. T., & Saar, M. O. 2019. A methodology to determine the elastic properties of anisotropic rocks from a single uniaxial compression test. *Journal of Rock Mechanics and Geotechnical Engineering*, 11(6), 1166–1183. <https://doi.org/10.1016/j.jrmge.2019.04.004>
- Talesnick, M. L., & Ringel, M. 1999. Completing the hollow cylinder methodology for testing of transversely isotropic rocks: torsion testing. *International Journal of Rock Mechanics and Mining Sciences*, 36(5), 627–639. [https://doi.org/10.1016/S0148-9062\(99\)00038-8](https://doi.org/10.1016/S0148-9062(99)00038-8)